Towards synchrotron-based nanocharacterization

Pierre Bleuet[1,3], Lucile Arnaud[4], Xavier Biquard[1,3], Peter Cloetens[3], Lise Doyen[4], Patrice Gergaud[1], Patrick Lamontagne[4], Maylis Lavayssière[1], Jean-Sébastien Micha[1,2,3], Olivier Renault[1], François Rieutord[1,3], Jean Susini[3] and Olivier Ulrich[1,3]

[1] *CEA, F38054 Grenoble, France*
[2] *CNRS-UMR 5819, F38054 Grenoble, France*
[3] *ESRF, F38043 Grenoble, France*
[4] *ST Microelectronics, Grenoble, France*

Abstract. The advent of 3rd generation synchrotron sources coupled with high efficiency x-ray focusing optics opened new nanocharacterization possibilities. This paper is an overview of synchrotron-based techniques that may be of interest for nanotechnology researchers. Although not exhaustive, it includes a general background of synchrotron principle and main x-ray interactions before addressing nanoimaging possibilities. Three-dimensional (3D) hard x-ray multimodal tomography is now doable that allows producing 3D morphological, chemical and crystalline images with a sub-100nm resolution. Although the resolution is still limited with respect to electron imaging, it presents attractive features like depth resolution and non-destructive exam. Besides imaging, diffraction also allows strain determination within microstructures and is illustrated here on 100nm copper lines. Surface analysis is illustrated through X-ray Photoelectron Emission Microscopy (XPEEM).

Keywords: Synchrotron, Tomography, Fluorescence, Diffraction, Strain, Spectroscopy.
PACS: 07.85.Qe, 07.85.Tt, 87.57.Q-, 87.64.kv, 87.64.Bx, 87.64.K-

INTRODUCTION

X-ray-based methods are very attractive for the nanotechnology user community willing to perform advanced characterization. This mainly comes from the fact that different experiments can be carried out on the very same setup for a particular set of samples, allowing to cross-check data and to validate physical processes. Until a few years back however, the use of x-rays for characterization was suffering from a lack of spatial resolution preventing nanoscale experiments.

With the advent of 3rd generation synchrotron sources and the development of excellent x-ray focusing optics, it now becomes possible to perform in-depth decananometer analyses using the large panel of x-ray characterization methods, most of them already existing and already validated but at a coarser scale.

In this paper, we review some of the main synchrotron x-ray tools that could benefit to the micro and nanoelectronics researchers. The paper is split as follows: the first section contains x-rays and synchrotron background and can be skipped for all those readers only interested in x-ray experimental possibilities. The second section is devoted to three-dimensional characterization by synchrotron radiation. This important section will be split into 3 subsections for morphological, chemical and crystalline imaging, respectively. After a brief introduction to coherent diffraction imaging in a third section, the fourth section addresses the problem of strain determination within microstructures using x-ray diffraction. The fifth section will deal with spectroscopic techniques dedicated to surface analyses.

Each time, the technique principle is briefly introduced and illustrated through experimental results, and limitations as well as perspectives are highlighted.

SYNCHROTRON AND X-RAY INTERACTION BACKGROUND

In this section we give the very basics of synchrotron radiation and interactions of x-ray with matter that will be the basis of all the techniques developed throughout this paper. It does not aim at giving an advanced course on accelerator physics but rather a general overview of synchrotron principle.

CP1173, *Frontiers of Characterization and Metrology for Nanoelectronics: 2009,*
edited by D. G. Seiler, A. C. Diebold, R. McDonald, C. M. Garner, D. Herr, R. P. Khosla, and E. M. Secula
© 2009 American Institute of Physics 978-0-7354-0712-1/09/$25.00

Downloaded 13 May 2010 to 159.226.100.225. Redistribution subject to AIP license or copyright; see http://proceedings.aip.org/proceedings/cpcr.jsp

Synchrotron radiation

To produce x-rays, one can purchase standard x-ray tubes that are based on the interaction between accelerated electrons and a metallic anode. When approaching the anode, electrons decelerate and the excess of energy is counterbalanced by the emission of polychromatic x-rays (so-called Bremsstrahlung effect) and highly monochromatic x-ray lines that are a signature of the anode material. Cooling down the anode while maintaining a stable beam remains a challenge that limits both flux and focusing possibilities. Rotating anodes are today the best way to produce x-rays with a brilliance of the order of 10^8-10^9 photons/s/mrad^2/mm^2/unit of bandwidth.

Instead of using the deceleration of electrons, synchrotrons are using the angular deviation of relativistic electrons. In a synchrotron, three stages are necessary to produce and store relativistic electrons. The pre-injector, consisting of an electron gun coupled to a *linear accelerator* allows reaching about 200MeV energy. This pre-injection step is mandatory to produce low emittance electron bunches. The high energy electron beam is further accelerated in a *booster* to reach 6GeV in the specific case of the ESRF machine [1]. The relativistic beam is then delivered to a large storage ring composed of *bending magnets* that act both as synchrotron sources and as a way to keep the electron path circular and *insertion devices*, which wiggles the beam to strengthen the brilliance. The word 'synchrotron' comes from the fact that the frequency of the acceleration voltage is synchronized with the electron bunches.

By deviating the electron beam from its original path, bending magnets are producing large, highly polychromatic x-ray beams with a medium brilliance (about 10^{16} brilliance unit). Those are well suited to spectroscopic experiments on highly concentrated samples requiring energy scans and also to any experiment requiring continuous polychromatic beams. Insertion devices -that can be either undulators or wigglers, mainly differing by the amplitude of the wiggles- produce an oscillation of the electron beam in a horizontal plane, reinforcing the x-ray beam brilliance that can reach 10^{20} brilliance unit for some dedicated energies. Insertion devices produce intense and narrow, nearly monochromatic beams with respect to bending magnets.

Once synchrotron x-rays are produced, they must be "processed" before being delivered to a sample. This is usually performed in a optics hutch, composed of several optical elements that filter out high harmonics, collimate the beam or use Bragg diffraction on Silicon monocrystals to produce monochromatic x-ray beams ($\Delta E/E=10^{-4}$). An experimental hutch, beamline specific and accessible to users, is used as the experimental end-station. Depending on beamline needs, it may provide focusing capabilities, large degree of freedom sample scanning and a panel of x-ray detectors specific to the interaction observed.

Main x-ray interactions

In this subsection we review some of the main interactions of x-rays with matter. Again, we do not aim at being exhaustive but rather briefly describing interaction processes that will be the basis for all the rest of the paper.

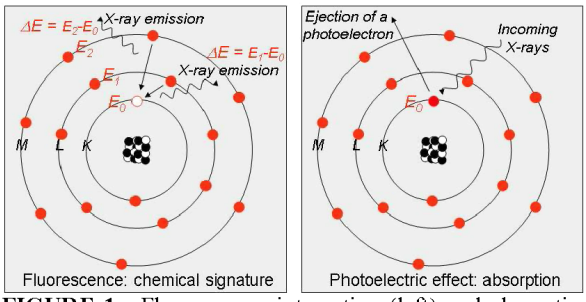

FIGURE 1. Fluorescence interaction (left) and absorption (right). In this figure, circles model electronic levels.

Fluorescence interaction (Fig. 1, left) occurs when a beam with sufficient energy ejects a core electron out of an atom. In turns, a set of fluorescence rays specific to each atom is produced. Fluorescence is typically used when trying to determine the unknown chemical composition of a sample or the quantitative distribution of minor elements, *e.g.* for contamination.

X-ray absorption (Fig. 1, right) is based on the absorption of an incoming beam by an atom, which in turns produces a photoelectron. This interaction is typically used in imaging techniques like radiography, tomography or spectroscopy. The photoelectron can also be used as a chemical signature for surface analyses.

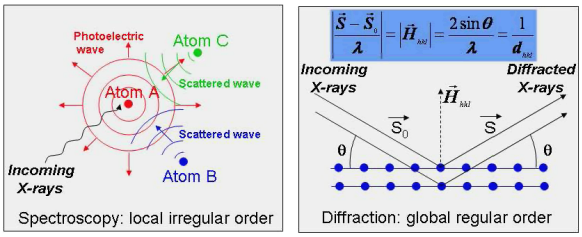

FIGURE 2. Spectroscopy (left) and diffraction (right). On the left image, the circles model a wave.

Spectroscopy (Fig. 2, left) is a less intuitive phenomenon that allows characterizing the local order of irregular structures by scanning the incoming beam energy and exploiting the interferences between waves emitted from neighbor atoms. Single or multiple

Downloaded 13 May 2010 to 159.226.100.225. Redistribution subject to AIP license or copyright; see http://proceedings.aip.org/proceedings/cpcr.jsp

interferences with other atoms may occur: in the case of X-ray Absorption Near Edge Spectroscopy (XANES), the excitation energy is slightly higher than the edge, leading to multiple interferences that create oscillations in the XANES spectra. In the case of Extended X-ray Absorption Fine Structure (EXAFS), the excitation energy is much higher than the edge, leading to single interferences.

Diffraction (Fig. 2, right) requires 'ordered' samples, *i.e.* periodic crystalline structures. The well-known Bragg law, detailed in Fig. 2, links the lattice, the Bragg angle and the wavelength. It can either be described analytically ($\lambda=2d\sin\theta$) or with vectors (see Fig. 2), in which case the incoming and outgoing vectors are linked to the vector H_{hkl} in the reciprocal space. Diffraction has a number of applications among which phase identification, thin film analysis, reflectivity or strain/stress determination.

THREE DIMENSIONAL DIRECT IMAGING TECHNIQUES

Introduction

Synchrotron x-ray tomography is very similar to medical scanners. The sample can be either fully illuminated and rotated in front of a wide beam, in which case the technique is often referred to as *transmission* or *projection* tomography, or the sample can be raster scanned along a linear path before being rotated in front of a focused beam, in which case the technique is referred to as *scanning* tomography. From the sampling scheme point of view, scanning tomography is identical to 1st generation medical scanners.

Although parallel beam microtomography is now widely used in most of synchrotrons, its resolution is detector-limited and turns out to be within a micrometer, although smaller voxel sizes may be obtained by the microscope. We don't detail here this now well-established technique, but rather a variation of it that aims at reaching higher resolution.

3D morphology

To overcome the detector resolution, an intense nearly monochromatic beam ($\Delta E/E=10^{-2}$) is focused down to less than 100nm [2]; the focal spot is used as a secondary x-ray source, with smaller dimensions, that allows to produce magnified radiographs thanks to the conic nature of the beam (Figure 3). Full details about this technique are given elsewhere [3, 4].

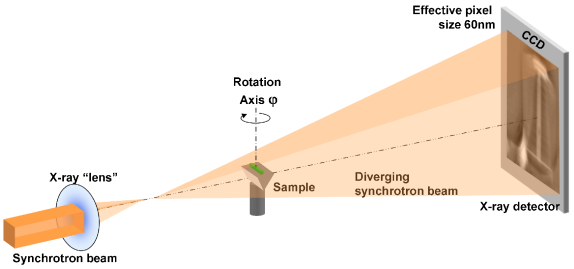

FIGURE 3. Projection geometry for tomography.

After specific pre-processing of the radiographs [5], standard reconstruction algorithms are used that, eventually, allow to produce 3D volumes sampled down to 60nm (Fig. 4). Those volumes are a distribution of the electron density of the object [5].

3D chemical imaging

Besides the global inner shape of a sample, it is interesting to get the 3D distribution of chemical elements within it. Fluorescence tomography has been developed years ago that allows to produce 3D chemical images at a resolution of a few micrometers [6,7].

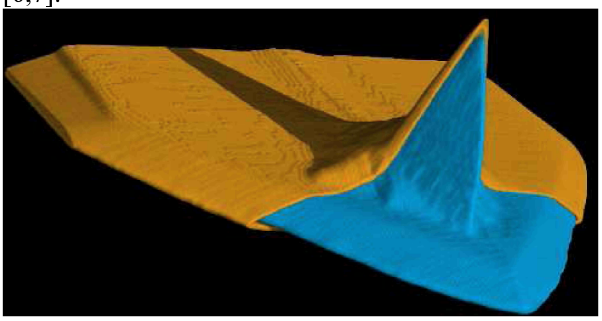

FIGURE 4. AFM (Pt,Ir) tip virtually split so that a lower density underlying region is identified [4]. The low density region is known to be Silicon, while the layer is known to be Pt as cross-checked by fluorescence tomography (Fig. 5). The vertical tip is about 12 micrometers high. Reprinted with permissions from [4]. Copyright 2009, American Institute of Physics.

Fluorescence mapping can be reproduced with smaller beams [8]. By keeping the scheme of Fig. 3 but bringing the sample right in the focal plane of the x-ray optics, one can switch to the so-called scanning geometry that consists in raster scanning the sample along a linear path, then rotating it by a fraction of a turn, and iteratively repeating those two steps until a full turn is completed. At each point, a fluorescence spectrum is recorded thanks to an energy dispersive detector placed at 90 degrees with respect to the x-ray beam (not represented on the figure, see [4]). Appropriate processing and reconstruction yields 3D,

Downloaded 13 May 2010 to 159.226.100.225. Redistribution subject to AIP license or copyright; see http://proceedings.aip.org/proceedings/cpcr.jsp

potentially quantitativively, reconstruction of the chemical elements within the volume (Fig. 5).

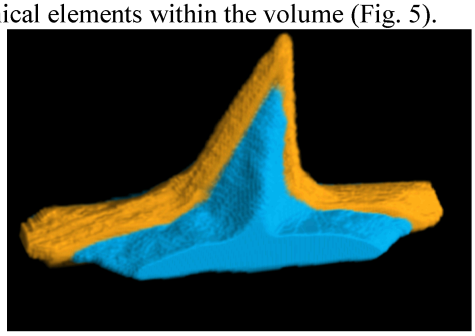

FIGURE 5. AFM (Pt,Ir) tip reconstruction, in scanning geometry.[4] In fluorescence tomography, chemical distribution is possible that allow distinguishing the Silicon (blue) from the Platinum (orange). Reprinted with permissions from [4]. Copyright 2009, American Institute of Physics.

3D crystalline imaging

Keeping the previous scanning geometry, it has been recently shown that crystalline depth-resolved imaging is possible that makes minor phase identification in powder-like samples possible.

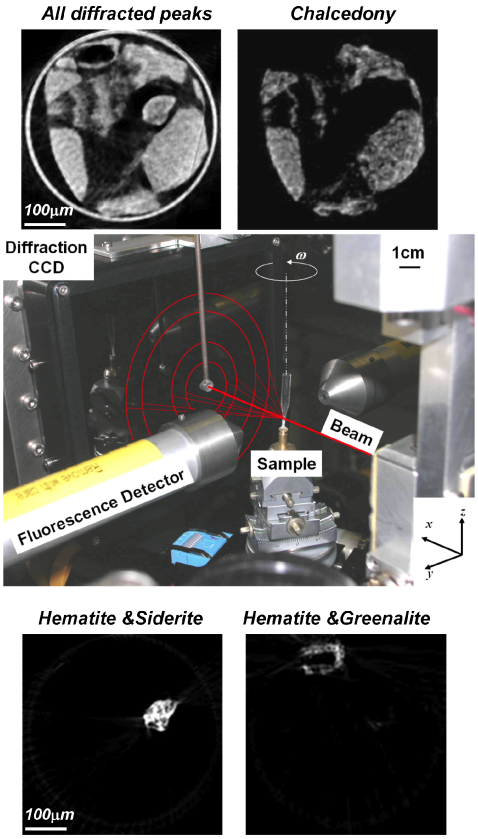

FIGURE 6. Diffraction tomography single-slice reconstructions of a sample made of different phases (top and bottom images, and a picture of the setup) [9].

Basically, the sample is in the focal plane and is raster scanned, similarly to fluorescence tomography, except that a new, on-axis CCD diffraction camera, is placed downstream from the sample [9,10]. Additionally to the imaging feature, a so-called reverse analysis allows to calculate back the local diffraction pattern coming from a single voxel, allowing to rise above of the standard detection limits of powder diffraction by few orders of magnitude [9]. At the sub-100nm scale, the method is still under commissioning. Few successful attempts have been realized; the main issues are coming from the fact that a sufficient number of crystallites must lie within the gauge volume, which is getting smaller with smaller beams. Therefore, samples may not behave like powders at 100nm scale, except for all those materials having a sufficiently high atomic numbers.

LENSLESS IMAGING

Lensless imaging is an attractive imaging method that can overcome resolution limitations of direct imaging. However, because we are mainly concerned by direct imaging methods, we just give here its general principle. Interested readers may refer to recent publications listed in the reference section [11-16].

Coherent Diffraction Imaging (CDI) was effectively implemented in 1999, though basic principle was enounced as early as 1980 [12,13]. Basically, the principle consists in illuminating a sample with a collimated, monochromatic, coherent, and soft x-ray beam, while recording on-axis diffraction patterns with a CCD camera located in the far-field propagation domain. It is somewhat easy to tune such an experimental setup with modern third-generation synchrotron sources. For non-crystallized samples the 'phase problem' can be overcome and image can be reconstructed, typically by applying support constraints all along an iterative process involving forward and backward Fourier transforms. The method presents outstanding features in terms of resolution, with respect to lens-based imaging techniques. For that reason, it is a very rapidly emerging technique and a number of recent papers have been published. Issues are *(i)* the trends to use of soft x-rays, which may not provide sufficient penetration depth for high atomic number samples, *(ii)* the reconstruction procedure that is based on a rather strong a priori knowledge about the sample shape *(iii)* rather long exposure time that may cause radiation damage and *(iv)* some restriction about the sample size, that must not be too big neither too small to get enough signal. Still, CDI produces unprecedented

Downloaded 13 May 2010 to 159.226.100.225. Redistribution subject to AIP license or copyright; see http://proceedings.aip.org/proceedings/cpcr.jsp

images that for sure will play a key role for nanocharacterization.

STRAIN DETERMINATION

Principle

Laue diffraction can be used to determine strain and stress distribution within micro-devices. Instead of using a monochromatic beam as described for the previous techniques, a polychromatic beam emanating from a bending magnet of the synchrotron storage ring can be used [17,18]. The hard x-ray polychromatic beam, about 20 keV wide, is focused down to 0.5x0.5 μm^2 using x-ray optics. The sample, tilted at 40degrees with respect to a horizontal plane, is raster scanned in one or two dimensions and Laue diffraction images are recorded onto a large area CCD camera placed above the sample.

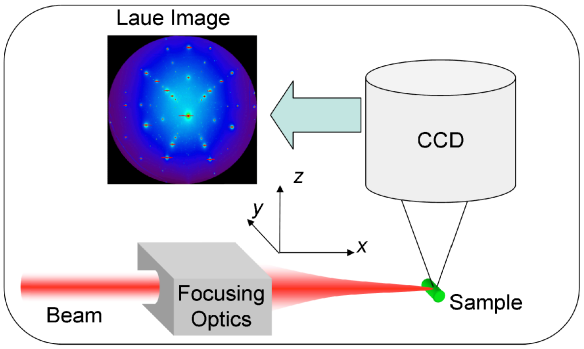

FIGURE 7. White beam diffraction setup.

In principle, a single Laue image allows to determine the local deviatoric strain tensor from which stress can be determined using elastic constants. The complete strain tensor can't be calculated from a single white beam diffraction image since the detector is not energy resolved, *i.e.* the energy of each diffracted spot can't be directly determined. Because of that, the strained lattice cannot be calculated and white beam diffraction only gives access to the deviatoric strain or stress; the hydrostatic component is not known. To get it, one has to switch to a monochromatic beam and identify the energy of the diffracted spots. Eventually, by combining both monochromatic and polychromatic analyses, the full strain tensor is determined.

Results

Here, we show preliminary results obtained in copper lines. Those copper lines are 100nm wide, 45 micrometers long and 220nm thick. It should be mentioned that Laue diffraction has never been reported on such small lines, to our knowledge.

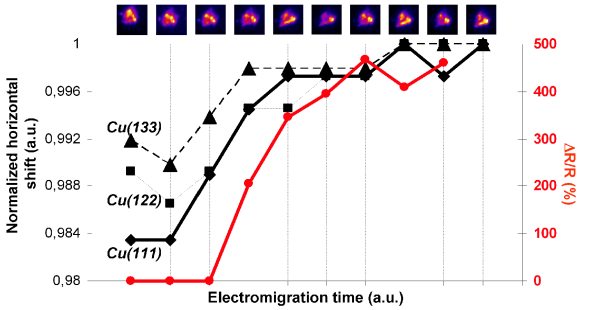

FIGURE 8. Evolution of diffraction spots during electromigration test. The red curve shows the normalized resistance while black curves (diamond, square, triangle) show the horizontal shift of the (111), (122) and (133) reflections, respectively. Cu(111) reflections can be seen at the top of the figure.

Copper lines are deposited on Silicon substrate. Experiment parameters are the following: white beam (5-22keV), spot size 1μm^2, commercial MAR CCD camera 2048x2048 with 16bits per pixels and a sample to detector distance of about 7cm. The sample is tilted to 40degrees with respect to the horizontal plane and scanned each micrometer across the line. To speed up the electromigration process, the sample temperature is fixed to 350°C using a commercial furnace from Anton-Paar. The current in the line is set to a constant value, and resistance measured all along the test. Identifying and indexing copper peaks has been performed using XMAS software [19]. Due to the rather weak signal coming from the 100nm lines, it turns out that finding and indexing spots was extremely sensitive to input parameters. Nevertheless, copper peaks could be isolated and indexed; their evolution has been tracked as shown on figure 8. In particular, we could observe a "rigid body" transformation of the diffraction pattern during the electromogration test: peaks are shifting all with the same amount and in the same direction, as illustrated on figure 8 with 3 reflections. It can also be seen that the peak shifting is correlated with the resistance evolution of the line, *i.e.* with the apparition of potential voids. This behavior demonstrates that the grains are rotating on themselves during the electromigration test. This observation, though not understood so far, is compatible with other work already published and appears to be typical of small copper lines [17].

SURFACE ANALYSES

X-rays potential mainly resides in the ability to observe in-depth effects. However x-rays can also be used to perform high resolution spectroscopic

Downloaded 13 May 2010 to 159.226.100.225. Redistribution subject to AIP license or copyright; see http://proceedings.aip.org/proceedings/cpcr.jsp

observations within the first few nanometers of a sample which open the ways to surface sensitive methods. X-ray photoelectron spectroscopy (XPS) is one of them and basically consists in irradiating a surface with a monochromatic x-ray beam with an incoming energy higher than that of the electron binding energies. Photoelectric effect occurs (Fig. 1) and photoelectrons are produced that can be recorded by a spectrometer giving chemical images, chemical and electronic states of elements within the sample. With respect to hard x-ray classical fluorescence experiments, XPS has the advantage to be extremely surface sensitive and low Z distribution can be reached, hydrogen and helium excluded. XPS with synchrotron radiation excitation offers invaluable opportunities in the field of surface studies of nanoelectronic materials [20-22]. X-ray Photoelectron Emission Microscopy (XPEEM) with energy-filtering has emerged recently with mature instruments [23,24] able to fully address the crucial need for high-spatial resolution of XPS in nanoelectronic research. Energy filtered-XPEEM with such aberration-corrected, high-transmission imaging spectrometers is intrinsically non-destructive, fast (full-field imaging) and allows simultaneously surface sensitive microscopy and spectroscopy. The technique enables true work-function imaging with laboratory sources at decananometric spatial resolution and tens of meV accuracy [25,26]; it makes possible XPS imaging (elemental and bonding state specific contrasts) with Al-Kα_1 excitation at a lateral resolution better than 650 nm, but which is limited by the low counting statistics arising from a still poor photon flux delivered by such sources.

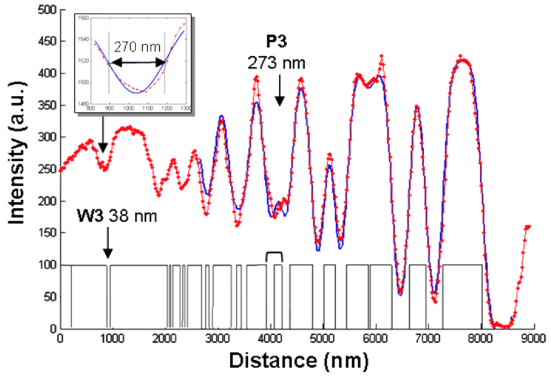

FIGURE 9. Lateral resolution measurements obtained in synchrotron-based energy dispersive XPEEM.

The much higher flux of synchrotron radiation is today the only way to overcome this limitation, but besides, soft x-ray excited XPEEM benefits from the energy tunability resulting in both sampling depth- and cross-section optimization. The technique already addressed several important issues such as the spectromicroscopy of doped silicon patterns and pn junctions [27,28], and the comprehensive analysis of single silicon nanowires [29]. We illustrate here the capabilities of synchrotron-based energy filtered XPEEM with the images in Fig. 9 of a cross-sectionned epitaxial semiconducting multilayer sample used for the measurement of lateral resolution and smallest-detectable object.

CONCLUDING REMARKS

X-rays present a number of elegant methods, potentially combinable. Absorption, fluorescence, spectroscopy and diffraction tools give nanotechnology researchers a wide range of possible diagnosis and characterization techniques. Synchrotrons, that are "just" ultra high brilliance x-ray sources, exploit those x-ray methods with additional features like reduced scanning time, coherence, tunable setup, techniques combination and easier *in-situ* experiment. Qualitative as well as quantitative measurement can be obtained in 3D and down to trace elements. Figure 10 summarizes the potential offered by synchrotron radiation.

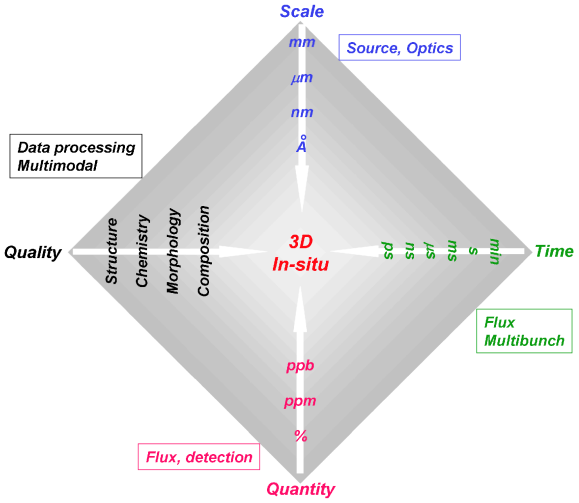

FIGURE 10. Sketch of synchrotron radiation potential.

Still, synchrotron radiation suffers from two main drawbacks. The first one is the resolution limitation that, for hard x-rays, limits experiments to a few tens of nanometers in the best case. The current synchrotron upgrade projects [30] mainly aim at pushing the limits of the instrument to produce truly nanometer beams within the next few years. As aforementioned, Coherent Diffraction Imaging is another alternative that will revolution x-ray nanoimaging. The second drawback is the access to synchrotron beamtime, which is getting more and more difficult because of a growing demand. To counterbalance this huge user demand, a number of

Downloaded 13 May 2010 to 159.226.100.225. Redistribution subject to AIP license or copyright; see http://proceedings.aip.org/proceedings/cpcr.jsp

synchrotrons covering various energy and resolution ranges have been built all over the world that hopefully may satisfy the researcher's needs [31]. Synchrotron is not in direct competition with electron microscopy: the two techniques are complementary. As such, synchrotron can be thought of as an additional tool integrated into a nanocharacterization process.

ACKNOWLEDGMENTS

The author would like to acknowledge the following people, some of them being involved in the results presented in this paper and already published and cited: M. Salomé, Nicolas Chevalier, Denis Mariolle, Eléonore Welcomme, Eric Doorhyée, Jean-Louis Hodeau, Philippe Walter, Rémi Tucoulou, Amal Chabli.

REFERENCES

1. Elleaume, P. "Future Storage Ring Synchrotron Sources", *in Synchrotron Radiation Instrumentation: Eighth International Conference on Synchrotron Radiation Instrumentation*, AIP Conference Proceedings **705**, American Institute of Physics, pp. 149-152 (2004).
2. Ortega, R., Cloetens, P., Devès, G., Carmona, A., and Bohic, S. PLoS One **2**, e925 (2007).
3. Mokso, R., Cloetens, P., Maire, E., Ludwig, W., and Buffière, J.Y. , *Appl. Phys. Lett.* **90**, 14 (2008).
4. Bleuet, P., Gergaud, P. Mariolle, D., Chevalier, N., Tucoulou, R., Susini, J., and Chabli, A., Rev. of Sci. Instr. **80**, 056101 (2009).
5. Cloetens, P., Ludwig, W., Baruchel, J., D. Van Dyck and J. Van Landuyt, Guigay, J-P., and Schlenker, M., *Appl. Phys. Lett.* **75**, 2912 (1999).
6. Kim, S.A., Punshon, T., Lanzirotti, A., Li, L., Alonso, J.M., and Ecker, J.R. , *Science* **314**, 1295 (2006).
7. B. Golosio, A. Somogyi, A. Simionovici, P. Bleuet, J. Susini, Appl. Phys. Lett. **84**, 122199 (2003).
8. Bleuet, P., Simionovici, A., Lemelle, L., Ferroir, T., Cloetens, P., Tucoulou, R., and Susini, J., *Appl. Phys. Lett.* **92**, 213111 (2008).
9. Bleuet, P., Welcomme, E., Dooryhée, E., Susini, J., Hodeau J-L., and Walter, P., *Nature Mat.* **7**, 468 (2008).
10. Stock, S.R., DeCarlo, F., Almer, J.D., *J Struct Biol* **161,** 144-150 (2008).
11. Pulizzi, F., *Nature Materials Insight* **8**, 259 (2009).
12. Sayre, D. *Acta Crystallogr.* **5**, 843 (1952).
13. Miao, J., Charalambous, P., Kirz, J., and Sayre, D., Nature **400**, 342-344 (1999).
14. Williams, G. J., Pfeifer, M. A., Vartanyants, I. A., and Robinson, I. K., *Phys. Rev. Lett.* **90**, 175501 (2003).
15. Chen, C-C., Miao, J., and Lee T. K., *Phys. Rev. Lett. B* **79**, 052102 (2009).
16. Pfeifer, M.A., Williams, G.J., Vartanyants, I.A., Harder R., and Robinson, I.K., Nature **442**, 63-66 (2006).
17. Budiman, A.S., Nix, W.D., Tamura, N., Valek, B.C., Gadre, K., Maiz, J., Spolenak, R., and Patel, J.R., *Appl. Phys. Letters* **88**, 233515 (2006).
18. N. Tamura, N., MacDowell, A. A., Celestre, R. S., Padmore, H. A., Valek, B., Bravman, J. C., Spolenak, R., Brown, W. L. *Appl. Phys. Letters* **80**, 3724 (2002).
19. Tamura, N., Celestre, R. S., MacDowell, A. A., Padmore, H. A., Spolenak, R. , Valek B. C., and Meier Chang, N., *Rev. Sci. Instr.* **73**, 1369 (2002).
20. Renault, O., Samour, D., Damlencourt J. F., Blin, D., Martin, F. Marthon, S. *Appl. Phys. Letters* **81**, 3627-3629 (2002).
21. Renault, O., Marlier, R., Gely, M., de Salvo, B., Baron, T., Hansson, M., Barrett, N. T., *Appl. Phys. Letters* **87**, 163119-163113 (2005).
22. Renault, O.; Fourdrinier, L.; Martinez, E.; Clavelier, L.; Leroyer, C.; Barrett, N.; Crotti, C., *Appl. Phys. Letters* **90**, 052112 (2007).
23. Escher, M., Weber, N., Merkel, M., Ziethen, C. , Bernhard, P., Schöhense, G., Schmidt, S., Forster, F., Reinert, F., Kröker, B., and Funnemann D., *J. Phys.: Condensed Matter* **17**, S1329 - S1338 (2005).
24. Renault, O., Barrett, N., Bailly, A., Zagonel, L. F., Mariolle, D., Cezar, J. C., Brookes, N. B., Winkler, K., Krömker, B., Funnemann, D. , *Surf. Sci.* **601**, 4727-4732 (2007).
25. Renault, O., and Chabli, A. "Energy-filtered Photoelectron Emission Microscopy (EF-PEEM) for imaging nanoelectronic materials,", AIP Conference Proceedings **931**, pp. 502-506 (2007).
26. Renault, O., Marlier, R., Barrett, N. T., Martinez, E., Baron, T., Gely, M., De Salvo, B., *Surface And Interface Analysis* **38**, 375-377 (2006).
27. Barrett, *J. Physics : Cond. Matter* to be published (2009).
28. M. Lavayssière *et al.* (this proceedings).
29. Bailly, A., Renault, O., Barrett, N., Zagonel, L.F., Gentile, P., Pauc, N., Dhalluin, F., Baron, T., Chabli, A., Cezar, J.C., Brookes, N.B., *Nano Letters* **8**, 3709-3714 (2008).
30. *European Synchrotron Radiation Facility: Science and Technology Programme 2008-2017*, available at http://www.esrf.eu/AboutUs/Upgrade/purple-book
31. http://www.lightsourcesorg

Downloaded 13 May 2010 to 159.226.100.225. Redistribution subject to AIP license or copyright; see http://proceedings.aip.org/proceedings/cpcr.jsp